euspen's 22nd International Conference & Exhibition, Geneva, CH, May/June 2022
www.euspen.eu

Electrochemical material removal characteristics of a NdFeB permanent magnet

Tom Petzold[1,*], André Martin[1], Andreas Schubert[1,2]

[1]*Chemnitz University of Technology, Institute for Machine Tools and Production Processes, Professorship Micromanufacturing Technology, Reichenhainer Str. 70, 09126 Chemnitz, Germany*
[2] *Fraunhofer Institute for Machine Tools and Forming Technology, Reichenhainer Str. 88, 09126 Chemnitz, Germany*

[*]*E-mail address of the submitting author: tom.petzold@mb.tu-chemnitz.de*

Abstract

Electric motors are used in various fields with an ever-increasing demand. In the electromobility sector as an example, a growth of a few hundred thousand motors per year is stated. In many cases, the rotor magnets for electric drives are produced by sintering. Special drives for two-axes positioning with precise movements require individual geometries of the rotor magnets such as spherical shapes. In this case, post-processing of the usually cylindrical or rectangular block shaped bar magnets is necessary.
One common technique for post-processing is electrical discharge machining (EDM), which allows the machinability of hard or brittle materials, but also causes thermal impacts, which influence the magnetic properties of the material in a negative way. To overcome this negative effect it is necessary to re-magnetize the rotor magnets after EDM. Additional measurements of the magnetic field strength are required to ensure correct values.
Electrochemical machining (ECM) represents an alternative technique for post-processing of rotor magnets, since it offers the possibility to avoid re-magnetization after the shaping process, because machining temperatures are well below the Curie temperature of most materials.
In this study, ECM of a NdFeB permanent-magnetic material is presented. The experiments were carried out according to DIN-SPEC 91399. The material-specific removal characteristics indicate an active dissolution with the chosen machining parameters. Comparative measurements of the magnetic field strength before and after ECM indicate that there is no negative influence of the removal process. The results suggest that ECM with pulsed current and oscillating tool cathode is an applicable technique for shaping rotor magnets.

Keywords: electrochemical machining, ECM, permanent-magnetic NdFeB, shaping of neodymium-iron-boron

1. Introduction

Electric motors are used in various fields, for example in automobile industry. Many electric motors consist of rotor magnets as functional driving components. In many cases, the rotor magnets are produced by sintering [1,2]. Special drives e.g. for two-axes positioning with precise movements require individual geometries of the rotor magnets such as spherical shapes [3]. In these cases, post-processing of the usually cylindrical or rectangular block shaped bar magnets is necessary. Due to the high hardness and the therefore related challenges of machining this material, one feasible process is electrochemical machining (ECM) [4].

Electrochemical machining is a process based on anodic dissolution of electrically conductive materials such as pure metals and metal-containing alloys. The process depends on the chemical properties of the sample material [5,6]. ECM has no thermal nor mechanical influence to the workpiece and due to the missing mechanical contact between tool and workpiece, no process-related tool wear occurs. Because of these facts, ECM offers the possibility to machine complex structures even in hard and difficult to machine materials such as NdFeB [7,8].

One further development of ECM is pulsed electrochemical machining (PECM). PECM enables improved electrolyte flushing due to an oscillation of the cathode and a pulsed current. The oscillation of the working gap allows high flushing rate when the gap is large while cathode is in the upper position and subsequently precise removal when the pulsed current is switched on in the lower position of the cathode [9,10].

The influence of the magnetic field in ECM was content of previous investigations, which focused on improvements of the electrochemical process. M. Baoji considered the improvement of localization for electrochemical machining by using a magnetic field [11]. He showed that it is possible to localize the anodic dissolution. Other researches analyzing the influence of an external magnetic field on the accuracy of the ECM process also showed that the magnetic field is useful for an increase in localization [12]. In the mentioned studies external magnetic fields were used to support or influence the ECM removals. Direct electrochemical machining of permanent-magnetic material with ECM is not known.

In this study, PECM of a permanent magnetic material of NdFeB was analyzed. The dissolution behaviour was characterized with experiments according to DIN-SPEC 91399. Resulting surface qualities of selected samples were measured. To identify influences on the magnetic properties of the workpiece, the magnetic field was measured before and after machining.

2. Experimental Setup and process parameters

The experiments were carried out on a PEMCenter 8000 with a custom device constructed for characterization of the

material-specific dissolution behavior according to DIN-SPEC 91399. The device consists of clamping systems for the tool cathode and the workpiece anode. ECM is carried out with a frontal working gap and a defined and constant machining area to be able to identify the resulting current densities from current measurements. The electrolyte is laterally flushed by a flushing chamber through the working gap. All mass removal experiments were carried out on the magnetic south pole of the samples.

The workpiece with its dimensions used for the experiments is shown in figure 1.

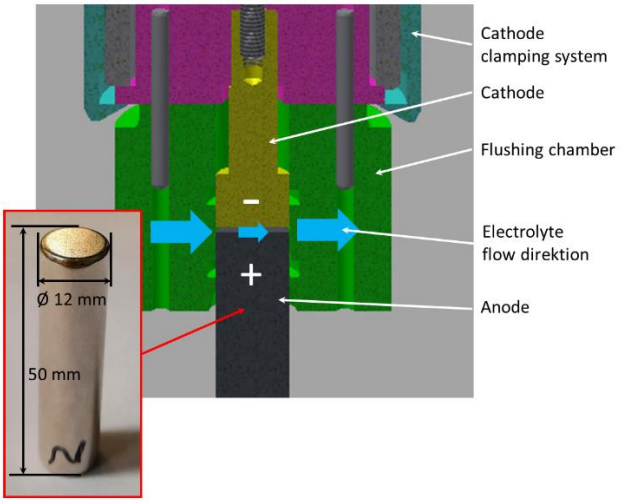

Figure 1. CAD model of the ECM device used for analysis of the removal characteristic with an unmachined sample

The samples for the characterization have a cylindrical shape with a diameter of 12 mm and a height of 50 mm as visible in figure 1. The mass fraction of the material is stated with $Nd_{28}Fe_{70}B_2$.

The specific removal mass m_{sp} of the NdFeB workpiece material was calculated according to equation (1)

$$m_{sp} = \sum_{i=1}^{n} w_i \cdot \frac{M_i}{z_i \cdot F} \quad (1)$$

The specific removal mass m_{sp} is the sum of every element in the alloy calculated with the quotient of the molar mass M, the chemical valence z and the Faraday constant multiplied with the mass fraction w of the respective element. The value for the specific removal mass m_{sp} for NdFeB is stated with 343 µg/C.

To measure the strength and orientation of the magnetic field of the samples before and after the experiments a PCE-MFM 3000 meter from PCE Instruments was used. The results show a magnetic field strength of approximately 460 mT ± 5 mT before machining.

The parameters used to machine the samples are charted in table 1. The parameters of the electrolyte and the initial working gap, pulse width and pulse frequency were kept constant. Voltage and feed rate are varied in the experiments to get different current densities.

Machining time and machining depth of the experiments are also varying depending on voltage and feed rate, but are not noted, because the termination criterion for the process is defined according to DIN-SPEC 91399 and was observed and kept for every single experiment.

Table 1 Process parameters for analysis of the material removal characteristic

Parameter	Value
Voltage U	(5 ... 14) V
Initial working gap s_A	50 µm
Electrolyte pressure ρ_{El}	300 kPa
Electrolyte type	Sodium nitrate
Electrolyte conductivity κ_{El}	70 mS/cm
Electrolyte temperature T_{El}	20°C
Feed rate v_f	(0.01 ... 0.4) mm/min
Pulse width t_p	4 ms
Pulse frequency f	50 Hz

The current efficiency η, for the analyses of the experiments, was calculated according to equation (2)

$$\eta = \frac{m_{ab}}{m_{sp} \cdot Q} \quad (2)$$

The current efficiency is the quotient of the removed mass m_{ab} and the product of the electric charge Q and the specific removal mass m_{sp}. Therefore, the electric charge of each experiment was calculated by integrating the process current I over the machining time t for each removal experiment according to equation (3).

$$Q = \int I dt \quad (3)$$

3. Results

The properties of the magnetic field were characterized again after the PECM experiments to detect influences from the machining process. The measurements showed 460 mT ± 5 mT, which was the same value as before machining. Thus, it can be stated that electrochemical machining had no influence on the magnetic field strength.

In figure 2 inclined top view images of the sample surfaces after machining with different current densities are shown.

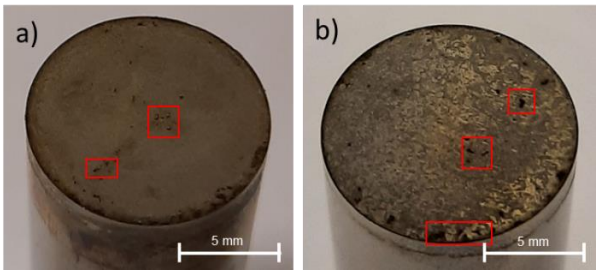

Figure 2. Surfaces of samples machined with different current densities; a) 10.0 A/cm²; b) 40.4 A/cm²

The surfaces of all machined samples are even and have no flushing marks. The surface of the sample shown in fig. 2 a) machined with a low current density looks smoother than the other ones. However, all sample surfaces are characterized by pits as marked by the red rectangles. This is expected to be caused by material inhomogeneities from the previous sintering process resulting in locally differing removal characteristics.

The machined surfaces were captured with a 3D laser scanning microscope VK-9700 from Keyence. Five parallel cross-sectional profiles were measured for each sample. The alignment of the profiles is shown exemplarily in figure 3.

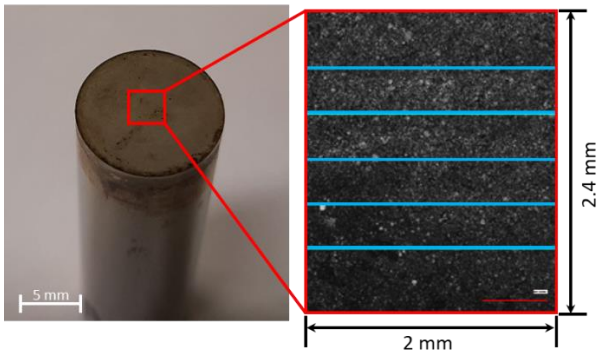

Figure 3. Representation of the surface quality measurement

The size of the measured field is 2 mm x 2.4 mm. The cross-sectional profiles are aligned horizontally with a distance of 350 µm to each other and have a length of 2 mm. The values of five profile lines were used to calculate an average roughness for every sample surface. The average roughness *Ra* and *Rz* are shown over the current density *J* in figure 4.

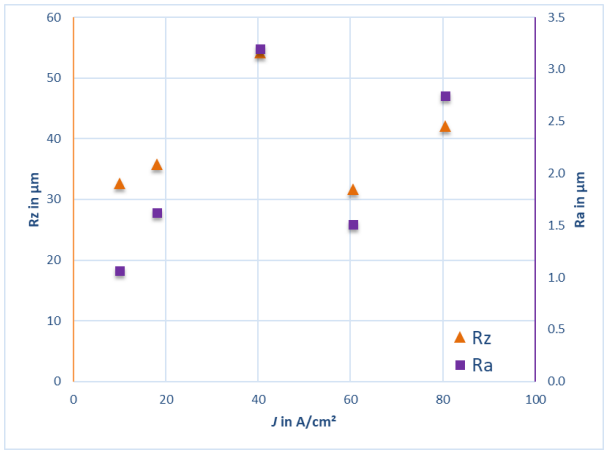

Figure 4. Roughness *Rz* and *Ra* over current density

The values for *Ra* are in the range from 1.06 µm to 3.19 µm. The values for *Rz* range from 31.6 µm to 54.3 µm. The lowest surface roughness of 1.06 µm *Ra* was measured at lowest current density of 9.97 A/cm², whereas the lowest value of 31.6 µm for *Rz* was measured at a mean current density of 60.5 A/cm². No systematic influence of the current density on the resulting roughness was detected.

The characteristic removal rate v_a depending on the current density is shown in figure 5.

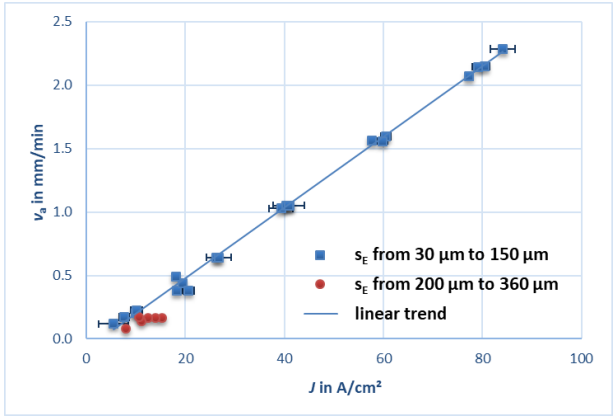

Figure 5. Removal rate as function of the current density of the material NdFeB for different gap size

The graph shows a linear behavior of the removal rate with increasing current density and a differentiation of the final working gap s_E. Because of this deviation the linear fit marked as blue line is only based on the data from the experiments with smaller working gaps marked with blue dots. The function of the linear fit is given in equation 4.

$$v_A = 0.028 \frac{\text{mm} \cdot \text{cm}^2}{\text{A} \cdot \text{min}} \cdot J - 0.068 \frac{\text{mm}}{\text{min}} \quad (4)$$

According to the diagram in fig. 5 the material was dissolved with removal rates up to 2.3 mm/min at current densities of 80 A/cm². For a successful mass removal, a minimum current density of 3.6 A/cm² is required.

In a range from 3 A/cm² to 20 A/cm² the experimental results with larger working gap (red dots) indicate that changing the current density only led to slight changes of the removal rate. It should be noted that the working gap was not adjusted before the experiments, but is a result of tool feed rate and chosen voltage and results as process parameter in equilibrium state. Therefore, only low current densities were possible with large working gaps between 200 µm and 360 µm as highlighted by the red dots in comparison to the smaller working gaps between 30 µm and 150 µm marked as blue rectangles.

Further analyses were carried out on the current efficiency η as function of the current density *J*. The results are presented in figure 6.

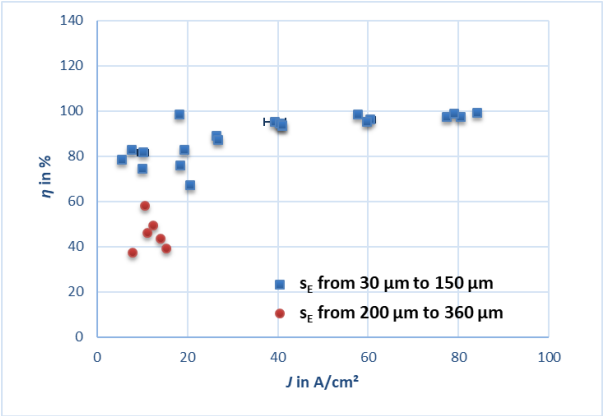

Figure 6. Current efficiency as function of current density

Figure 6 shows a significant difference between experiments with small and those with large working gaps. The current efficiencies for experiments with small gaps range from 75 % at low current density to 100 % at higher current density. The experiments with current densities below 60 A/cm² show a current efficiency between 75 % and 93 %, which is a trans-passive dissolution behavior, but for experiments with current densities higher than 60 A/cm², current efficiencies between 96 % and 99 % were found, which represents active dissolution behaviors. The experiments with larger gaps are all located in the range from 3 A/cm² to 20 A/cm² with current efficiencies between 40 % and 60 %.

4. Summary

The material-specific electrochemical removal characteristic of NdFeB was determined with sodium nitrate electrolyte at an electric conductivity of 72 mS/cm. A linear increase of the removal rate over the current density was found. The permanent-magnetic material shows a trans-passive dissolution behaviour at current densities below 60 A/cm², whereas at higher current density an active material removal behaviour was found. In the range from 3 A/cm² to 20 A/cm² the removal

behaviour significantly depends on the working gap size, which leads to a wide variation of the current efficiency.

The magnetic field strength was not influenced by the electrochemical machining process as shown by comparative analyses before and after PECM. The roughness of the samples ranges from 1.06 µm to 3.19 µm of *Ra* and from 31.6 µm to 54.3 µm of *Rz*. There was no systematic influence of the current density on the roughness values.

In future researches the material removal characteristic of NdFeB in non-magnetic state will be determined and compared to the removal characteristic of the permanent-magnetic material to identify influences of the magnetic field. Further experiments are planned on PECM for shaping geometrically pre-defined rotor-magnets.

References

[1] Sugimoto, S.: Current status and recent topics of rare-earth permanent magnets, Journal of Physics D: Applied Physics, Vol. 44, 2011

[2] Brown, D.; Ma, B.-M.; Chen, Z.: Developments in the processing and properties of NdFeB-type permanent magnets, 2002, DOI: 10.1016/S0304-8853(02)00334-7

[3] Yan, L.; Chen, I-M.; Lim, C.K.; Yang, G.; Lin, W.; Lee, K.-M.; Design and Analysis of a Permanent Magnet Spherical Actuator, IEEE/ASME Transactions on Mechatronics Vol. 13, 2008, DOI: 10.1109/TMECH.2008.918573

[4] Meichsner, G.; Hackert-Oschätzchen, M.; Krönert, M.; Edelmann, J.; Schubert, A.; Hahn, G.; Putz, M.: Characterisation of the Influence of Material Hardness in Precise Electrochemical Machining of Steel, In: Proc. of the 17th International Conference on the Strength of Materials (ICSMA 17), 2015, ISBN 978-80-87434-07-9

[5] Meichsner, G.; Hackert-Oschätzchen, M.; Krönert, M.; Edelmann, J.; Schubert, A.; Putz, M.: Fast Determination of the Material Removal Characteristics in Pulsed Electrochemical Machining, In: Procedia CIRP, 7th HPC 2016 – CIRP Conference on High Performance Cutting, Volume 46, 2016, S. 123-126, DOI:10.1016/j.procir.2016.03.175

[6] C. Rosenkranz. Elektrochemische Prozesse an Eisenoberflächen bei extremen anodischen Stromdichten. Dissertation, Heinrich-Heine-Universität Düsseldorf, 2005.

[7] Klocke, F.; König, W.: Fertigungsverfahren 3; Abtragen, Generieren und Lasermaterialbearbeitung. Springer-Verlag, 2007, ISBN 978-3-540-48954-2

[8] Wilson, J.F.: Practice and Theory of Electrochemical Machining. New York: Wiley-Interscience, 1971, ISBN-13: 978-0471949701

[9] C. Rosenkranz, M.M. Lohrengel, J.W. Schultze. The surface structure during pulsed ECM of iron in NaNO3. Electrochimica Acta, 50:2009-2016, 2005.

[10] R. Förster. Untersuchung des Potentials elektrochemischer Senkbearbeitung mit oszillierender Werkzeugelektrode für Strukturierungsaufgaben der Mikrosystemtechnik. Cuvillier, 2004. ISBN3-86537-228-7.

[11] Lilong, Baoji M, Cheng P, Yun K, Yin P, Effect of magnetic field on the electrochemical machining localization, International Journal of Advanced Manufacturing Technology (2019) 102:949-956

[12] Ma B J, Fan Z J, Stephenson D J, Influence on Magnetic Flied Distribution on ECM Process, Key Engineering Materials (Volume 339), 2007, S.50-58